POLITECNICO DI TORINO
Repository ISTITUZIONALE

Corrosion Behaviour of Zr-Ag Alloys for Dental Implant Application

(Article begins on next page)

11 February 2024

![Scientific Research Publishing]

Corrosion Behaviour of Zr-Ag Alloys for Dental Implant Application

Francesco Rosalbino[1*], Daniele Macciò[2], Giorgio Scavino[1]

[1]Dipartimento di Scienza dei Materiali e Ingegneria Chimica (DICHI), Politecnico di Torino, Torino, Italy
[2]Dipartimento di Chimica e Chimica Industriale (DCCI), Università Degli Studi di Genova, Genova, Italy
Email: *francesco.rosalbino@polito.it

Abstract

The electrochemical corrosion behaviour of three Zr-Ag alloys (Zr-1Ag, Zr-3Ag and Zr-5Ag) was investigated. Open circuit potential, linear potentiodynamic polarization and electrochemical impedance spectroscopy (EIS) techniques were employed in aerated artificial saliva (pH = 4.0) at 37°C. Silver alloying additions are found to be effective in enhancing the corrosion resistance of zirconium in artificial saliva environment. In fact, Zr-Ag alloys exhibit higher open circuit potentials, larger breakdown potentials and higher impedance values as compared to cp Zr. This behaviour can be ascribed to the formation of a thicker and more stable passive film with increasing compactness, able to provide better protection against the corrosion attack.

1. Introduction

Zr is a valve metal characterized by very high stability in several aggressive environments and Zr alloys have been successfully employed in biomedical applications owing to their greater strength, lower cell cytotoxicity, lower magnetic susceptibility than titanium and excellent hemocompatibility [1] [2]. Moreover, *in vivo* evidences have indicated that zirconium implants exhibit good osteointegration [3] [4] and studies comparing zirconium and titanium implants showed that the degree of bone-implant contact is higher in the case of zirconium [5] [6]. The advantageous Zr behaviour *in vitro* and *in vivo* has been ascribed to the presence of a protective surface oxide layer that reduces the corrosion rate, the-

reby minimizing ion release in bioenvironments and facilitating the osteointegration process [7] [8]. Based on these characteristics, Zr and its alloys have been proposed as candidates for permanent implants [1].

The oral cavity represents a very aggressive environment for metallic materials and the corrosion resistance is a fundamental factor in assessing their role as dental implants. In fact, the release of ions deriving from the corrosion of a metal or alloy stimulates the growth of macrophages. Moreover, a rough surface on the corroded metal promotes the adhesion of bacteria and the formation of plaque, which can induce periodontitis and gingivitis [9]. Furthermore, the fatigue failure of dental implants appears to be intimately related to the corrosion of metallic material [10] [11]. Though zirconium exhibits high corrosion resistance in acid or alkali media, it is susceptible to localized corrosion induced by chloride ions [12] [13]. Consequently, it would be of great importance to develop Zr alloys with a higher corrosion resistance in the oral environment since saliva typically presents concentrations of ca. 0.15 mass % Cl^- [14].

Recently, it has been reported that silver plays an important role in improving the corrosion resistance of titanium alloys in biological environments [15] [16] [17] [18]. The beneficial effect of silver is attributed to its higher standard electrode potential ($E_0 = 0.799$ V) than titanium ($E_0 = -0.98$ V), which promotes the formation of stable titanium oxide film. Ag has excellent corrosion resistance in many aqueous solutions, and good in vivo biocompatibility. Some dental amalgams added with Ag have been successfully used as dental materials [19].

Aim of the present work is to assess the corrosion behaviour of various Zr-Ag alloys with different compositions during exposure to artificial saliva environment. For the sake of comparison, cp Zr was also investigated in the same experimental conditions. The study was carried out using open circuit potential, linear potentiodynamic polarization and electrochemical impedance spectroscopy techniques in order to assess the potential ranges for the stability of the investigated materials, and to evaluate the resistance of the passive films formed on their surface.

2. Experimental Details

Zr-Ag alloys (Zr-1Ag, Zr-3Ag, Zr-5Ag, *mass* %) were prepared starting from zirconium (99.999 *mass* %) and silver (99.9 *mass* %). Calculated amounts of the elements were weighed with an accuracy of 0.01 mg and arc-melted on a water-cooled copper plate under argon atmosphere. The samples were re-melted twice for homogenization, and possible mass losses were generally found to be negligible. A scanning electron microscope EVO 40 (Carl Zeiss), equipped with a Pentafet Link (Oxford Instruments) detector for EDXS analysis was used to examine the microstructures and measure alloy composition prior to electrochemical tests.

The Zr-Ag samples were made into electrodes by inserting insulated copper wires and protecting all sides but one with epoxy resin. Before the electrochemi-

cal characterization, all specimens were pre-treated by mechanical polishing of the electrode surface up to a mirror finish. The exposed geometric area was 0.5 cm^2.

Electrochemical measurements were performed in Fusayama artificial saliva (0.4 g NaCl, 0.4 g KCl, 0.795 g CaCl$_2$, 0.69 g NaH$_2$PO$_4$, 0.005 g Na$_2$S, 1 g urea, and distilled water up to 1000 ml). The pH of the aggressive environment was adjusted to 4.0 by adding lactic acid in order to simulate physiological conditions representative of what a biomedical component would experience [20] [21] [22] [23]. The artificial saliva was naturally aerated and the experiments were conducted without stirring. The temperature was maintained at 37˚C ± 1˚C using a thermostatic bath. Electrochemical measurements were performed using a conventional three-electrode glass cell with a large platinum sheet and a saturated calomel electrode (SCE) serving as the counter and the reference electrodes, respectively. The Zr-Ag alloys were studied in as-cast conditions.

Linear potentiodynamic polarization curves were recorded starting from −1000 mV/SCE and moving in the electropositive direction at a scan rate of 0.5 mV/s, after allowing a steady-state potential to develop. Open circuit potential, E_{OC}, was measured with respect to the SCE every minute for a period of 2 h. All stationary measurements were performed using a Solartron 1286 Electrochemical Interface controlled by a personal computer.

Electrochemical impedance spectroscopy (EIS) measurements were carried out on the specimens subjected to various potential condition while exposed to artificial saliva. An EG&G PAR system Model 2263 driven by a computer was employed for EIS measurements using 10 mV amplitude of sinusoidal voltage over a frequency range extending from 100 kHz to 10 mHz at seven points per decade. First EIS spectra were acquired at the open circuit potential attained by the samples after 2 h exposure to the aggressive environment. Next, the potential was set at +500 mV/SCE for 30 min before recording the EIS spectra of the polarized specimen. Experimental data were stored in the computer and processed according to the EQUIVCRT program (B.A. Boukamp, University of Twente).

For comparison, electrochemical experiments were also performed on cp Zr supplied by Johnson Matthey, London, UK.

3. Results and Discussion

The open circuit potential, E_{OC}, variations vs. exposure time of pure Zr and Zr-Ag alloys in artificial saliva, for a period of 2 h are reported in Figure 1. The time profiles of E_{OC} obtained for the investigated samples are typical of passive metals exposed to aerated solutions. For cp Zr, the initial open circuit potential is −850 mV (SCE), then it gradually changes towards more positive values and after 2 h of exposure a potential of −700 mV (SCE) is reached. The time profiles of E_{OC} obtained for the Zr-Ag alloys are quite similar. The initial E_{OC} for the Zr-1Ag alloy is −770 mV (SCE), then it progressively increases to nobler potentials reaching after 2 h a steady value of about −625 mV (SCE). For the Zr-3Ag alloy, the initial open circuit potential is −690 mV (SCE), then it gradually
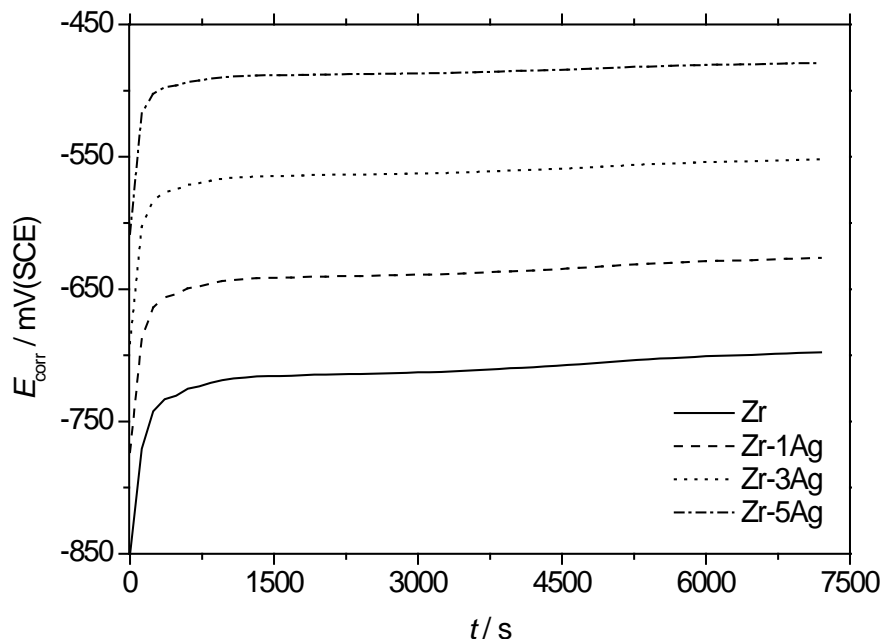
Figure 1. Open circuit potential vs. time profile for cp Zr and Zr-Ag alloys after 2 h exposure to aerated artificial saliva, pH = 4.0.

increases and after 2 h exposure a steady value of nearly −550 mV (SCE), is reached. The initial E_{OC} value for the Zr-5Ag alloy is −605 mV (SCE), then it increases progressively and after 2 h of immersion it remains stable at approximately −480 mV (SCE). The observed behaviour indicates that all the Zr-Ag alloys studied as well as cp Zr undergo spontaneous passivation due to the formation of an oxide film passivating the metallic surface, in artificial saliva solution.

Similar behaviour was found by Zhang *et al.* [20], where an initial increase in the E_{OC}s during the early minutes followed by stabilization observed on all the specimens (cp Ti and Ti-Ag alloys) suggests that a protective film formed rapidly on the metal surfaces in artificial saliva solutions and remained stable during the entire period of immersion (4.5×10^3 s) [24].

The initial E_{OC} increase observed for both cp Zr and Zr-Ag alloys can be ascribed to the thickening of the oxide film formed at the specimen surface, thereby improving its corrosion protection ability in artificial saliva. The open circuit potential increases until the oxide layer reaches its limiting protective capacity, thus resulting in stabilization of E_{OC} [25] [26].

As can be seen in **Figure 1**, Zr-Ag alloys exhibit higher E_{OC} values with respect to cp Zr, suggesting that silver alloying additions enhance the protection characteristics of the oxide layer, thus rendering the Zr alloys less prone to corrosion compared to cp Zr.

Figure 2 shows the potentiodynamic polarization curves of cp Zr and Zr-Ag alloys recorded in aerated artificial saliva at 37°C. No active-passive transition is observed on the anodic branch of polarization curves, confirming the passive
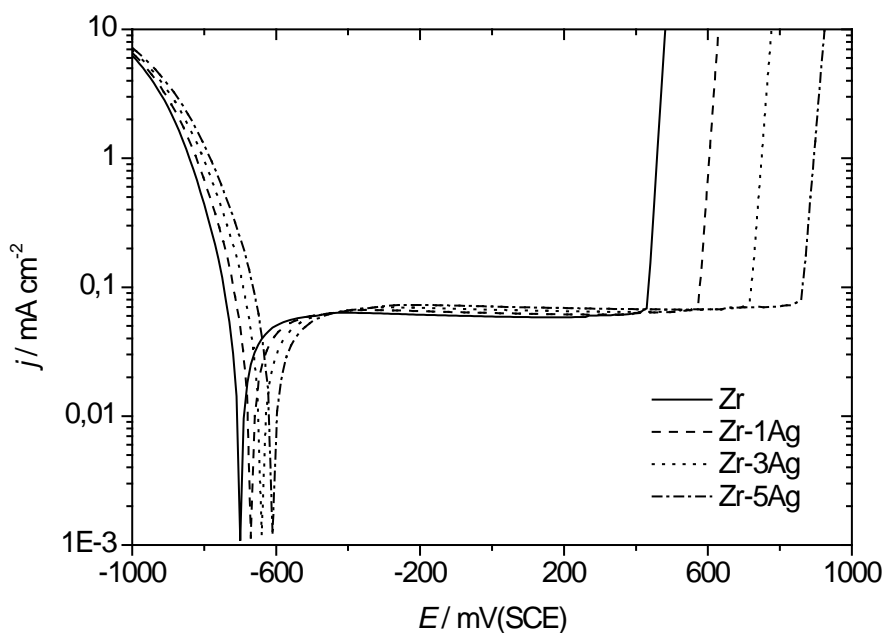
Figure 2. Potentiodynamic polarization curves of cp Zr and Zr-Ag alloys in aerated artificial saliva, pH = 4.0.

behaviour of specimens in the aggressive environment pointed out from the E_{OC} measurements. Both cp Zr and Zr-Ag alloys exhibit a passive potential range, ascribed to the formation and growth of a stable and protective oxide film, followed by a sharp increase in current density indicating breakdown of passivity and rapid growth of pitting.

Table 1 reports the values of the corrosion, E_{corr}, and breakdown, E_b, potentials found for the materials investigated, together with the extent of passive range, $\Delta E = E_b - E_{corr}$, which provides a reliable measure of the breakdown resistance [27] [28]. Based on these data, the corrosion resistance of cp Zr and Zr-Ag alloys in artificial saliva can be assessed. The corrosion potentials determined from the polarization curves are lower than those derived from E_{OC} measurements. This is expected since polarization curves start at a cathodic potential of −1000 mV/SCE, therefore the passive film at the surface of samples is partially removed owing to the highly reducing initial potential. As can be seen, addition of increasing silver content leads to a positive shift of the corrosion potential, confirming the previous E_{OC} measurements. Moreover, the breakdown potential progressively shifts towards more noble values and the extent of passive range gradually increases. Hence, increasing silver amounts progressively enhance the electrochemical stability of the oxide film, thus reducing the susceptibility to localized corrosion. Since the natural potential of human body ranges from +400 to +500 mV (SCE) [29], the potential for breakdown of the passive film achieved by all Zr-Ag alloys in artificial saliva can be regarded safe enough for these materials to be proposed for dental implant.

Figure 3 reports the EIS spectra, in the form of Nyquist diagrams, of cp Zr and Zr-Ag alloys at open circuit potential, after 2 h exposure to aerated artificial

Table 1. Corrosion potential, E_{corr}, breakdown potential, E_b, and extent of passive range, ΔE, for cpZr and Zr-Ag alloys determined by analysis of the anodic part of the polarization curves recorded in aerated artificial saliva at 37˚C.

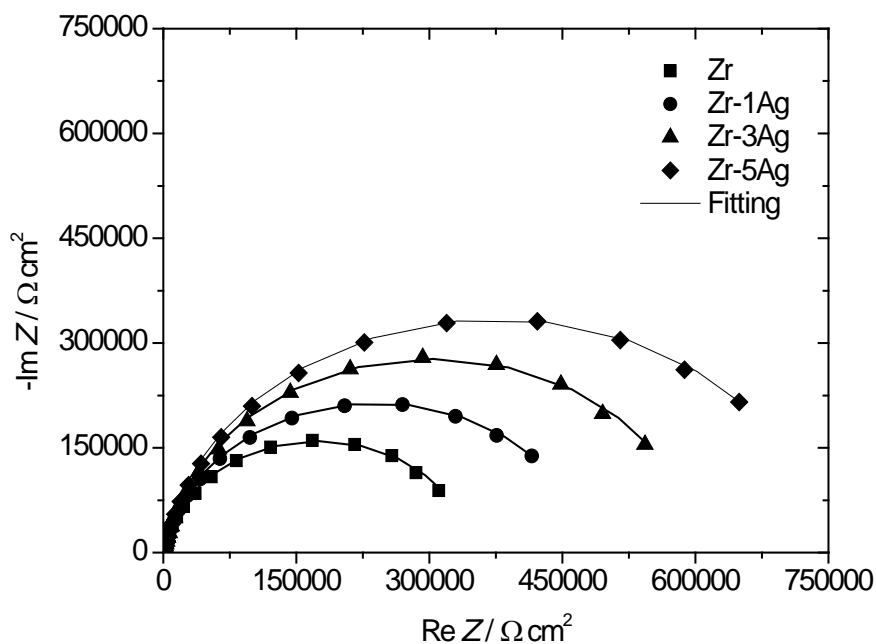| Sample	E_{corr} (mV)	E_b (mV)	$\Delta E = |E_{corr} - E_b|$ (mV)
Zr	−700	420	1120
Zr-1Ag	−665	570	1235
Zr-3Ag	−640	700	1340
Zr-5Ag	−610	840	1450

Figure 3. Experimental and simulated Nyquist diagrams for cp Zr and Zr-Ag alloys after 2 h exposure to aerated artificial saliva, pH = 4.0.

saliva at 37˚C. All Nyquist diagrams present depressed and incomplete capacitive semicircles, however cp Zr exhibits lower impedance values as compared with Zr-Ag alloys, the highest values being measured for the Zr-5Ag alloy. These results confirm an increase in corrosion resistance of zirconium related to silver alloying additions, in agreement with the results obtained from open circuit potential and potentiodynamic polarization measurements.

The zirconium/aggressive environment interface can be described by several equivalent circuit models, depending on the structure of the oxide film. The existence of a compact oxide film is represented by an equivalent circuit with one time constant [13] [30] [31], whereas for a porous film, a circuit with two time constants is employed [32] [33] [34].

Both cp Zr and Zr-Ag alloys characterized by EIS at their open circuit potential can be described by an equivalent circuit model with one time constant, and good agreement between experimental data and fitted data is obtained. The proposed equivalent circuit, shown in **Figure 4**, assumes that the corrosion of
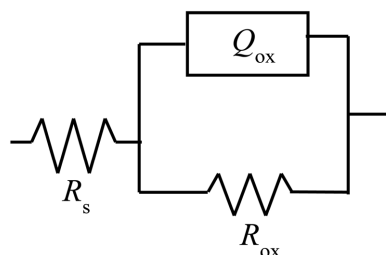
Figure 4. Proposed equivalent circuit for modeling experimental impedance data performed after 2 h exposure to artificial saliva, pH = 4.0.

the passive metallic material is hindered by the presence of a surface oxide film that acts as a barrier-type compact layer [13] [30] [31]. The equivalent circuit consists of a series combination of the aggressive environment resistance, R_s, and a single parallel constant phase element/resistor pair, Q_{ox}/R_{ox}, describing the properties of the passive film formed on the investigate materials, respectively the capacitance and resistance of the compact oxide layer.

A constant phase element, CPE, was used for fitting the impedance spectra instead of a pure capacitance owing to the non-ideal capacitive response due to the distributed relaxation feature of the oxide film. The impedance of the CPE is given by:

$$Z_{CPE} = \left[Y_0 \left(j\omega \right)^n \right]^{-1} \tag{1}$$

where Y_0 is a constant, $j^2 = -1$ is the imaginary number, ω is the angular frequency and $-1 \leq n \leq 1$. The value of n seems to be associated with the non-uniform distribution of current as a result of roughness and surface defects [35].

Analysis of the EIS spectra in terms of the equivalent circuit shown in **Figure 4** allows the parameter Q_{ox} and R_{ox} to be determined, and their values are reported in **Table 2**. The agreement between experimental and simulated data indicates that the experimental impedance spectra are well fitted to the proposed equivalent circuit. The fitting quality was evaluated by chi-squared (χ^2) values of about 10^{-4}, with a relative error less than 5%. On the Nyquist plots in **Figure 3**, the experimental data are shown as individual points, while the fitted spectra are presented as continuous lines.

Capacitance values of the passive oxide film can be extracted from the CPE parameter, Q_{ox}, using [36]:

$$C_{ox} = \left(R_{ox}^{1-n} Q_{ox} \right)^{1/n} \tag{2}$$

and are given in **Table 2**.

Comparing the capacitances for cp Zr and Zr-Ag alloys samples, it is possible to observe that pure zirconium has the highest capacitance value (about 82 μF cm^{-2}) when compared with that of the Zr-Ag alloys. This indicates a better capacitive effect of the oxide layers formed on Zr-1Ag, Zr-3Ag, Zr-5Ag specimens

Table 2. Electrical parameters of the equivalent circuit for cpZr and Zr-Ag alloys in aerated artificial saliva, pH = 4.0, at 37˚C. AC polarization was applied at their corresponding open circuit potential values in the aggressive environment.

Sample	Q_{ox} (10^5 S cm^{-2} s^n)	n	R_{ox} (Ω cm^2)	C_{ox} (F cm^{-2})
cpZr	1.5	0.87	3.45×10^5	8.17×10^{-5}
Zr-1Ag	1.3	0.88	4.90×10^5	6.53×10^{-5}
Zr-3Ag	1.2	0.89	6.30×10^5	4.78×10^{-5}
Zr-5Ag	1.1	0.90	7.75×10^5	2.94×10^{-5}

and, assuming a similar dielectric constant for such oxides, an increasing film thickness [37] [38], thereby confirming the previous E_{OC} measurements. As can be seen in **Table 2**, both cp Zr and Zr-Ag alloys exhibit high R_{ox} values, >10^5 Ω cm^2, indicating high corrosion resistance of these materials in artificial saliva. The presence of protective passive film provides the high corrosion resistance of specimens in this aggressive environment. However, the resistance of the oxide layer formed on cp Zr is lower than that measured for Zr-Ag alloys, the highest value being observed for the Ti-5Ag alloy. Low capacitances combined with high resistances suggest that the spontaneously formed passive film on Zr-Ag specimens becomes more compact and isolating on increasing the silver content in the alloy, affording better protection of the electrode surface against corrosion in artificial saliva.

EIS measurements were also carried out on the specimens polarized at +500 mV/SCE and the corresponding Nyquist plots are shown in **Figure 5**. By considering the impedance values two different behaviours can be distinguished: 1) Zr-Ag alloys exhibit higher impedances under anodic polarization than at the open circuit potential; and 2) cp Zr displays the opposite trend. The enhanced impedance showed by Zr-Ag alloys is indicative of additional growth of the passive film favoured by anodic oxidation. In this case, the impedance spectra can be satisfactorily fitted with the equivalent circuit reported in **Figure 6**, which is widely used to represent a bilayer structure of the anodic oxide films grown on valve metals such as Zr [39] [40] [41] [42]. The model assumes that the duplex structure consists of a barrier-type compact inner layer and a porous outer layer. The equivalent circuit includes the solution resistance, R_s, in series with two parallel constant phase element/resistor pairs, Q_p/R_p and Q_b/R_b, where R_p corresponds to the resistance of the porous layer, R_b to the resistance of the barrier layer, Q_p to the capacitance of the porous layer and Q_b to the capacitance of the barrier layer. A constant phase element, Q, representing a shift from the ideal capacitor was employed instead of the capacitance itself. A very good correlation between the fitted and the experimental data is also obtained for the polarized specimens. The values of fitted parameters are reported in **Table 3**. It can be seen that the values of R_b are significantly higher than those determined for R_p, indicating that the protection provided by the passive oxide film is predominantly due to the compact inner layer.
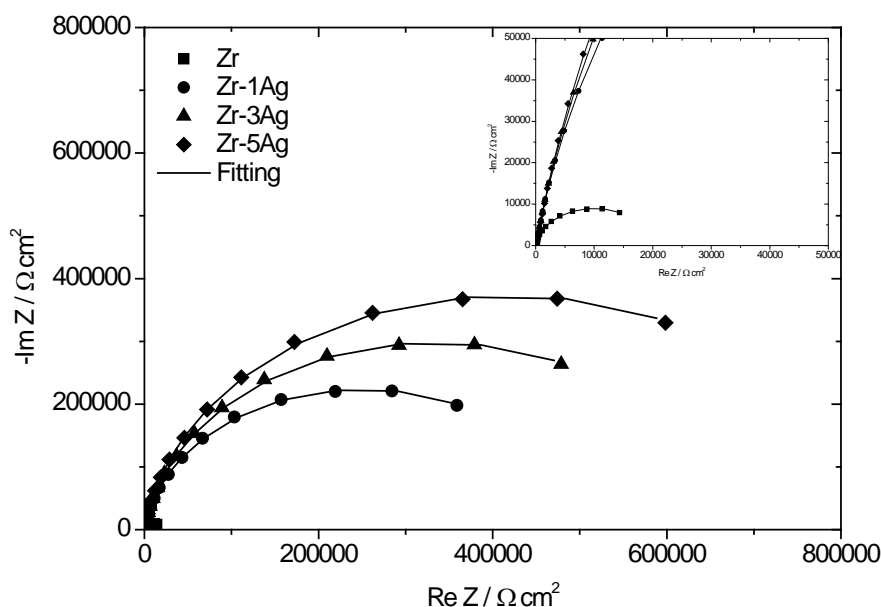
Figure 5. Experimental and simulated Nyquist diagrams for cp Zr and Zr-Ag alloys polarized at +500 mV/SCE during exposure to aerated artificial saliva, pH = 4.0.
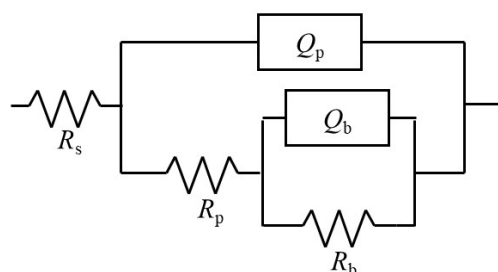

Figure 6. Proposed equivalent circuit for modeling experimental impedance data performed after polarization at +500 mV/SCE of Zr-Ag alloys in artificial saliva, pH = 4.0.

On the contrary, cp zirconium exhibits smaller resistances, over one order of magnitude, as compared to Zr-Ag alloys when anodically polarized, indicating a thinning of the oxide film or even losses of the film continuity attributable to localized corrosion phenomena. This means that the oxide film spontaneously formed at the surface of this sample at E_{oc} during exposure to artificial saliva becomes instable during application of +500 mV (SCE). Accordingly, the underlying metal is directly exposed to the aggressive environment and corrodes in artificial saliva. In this case, a good agreement between fitted and experimental data is attained with the electrical model reported in **Figure 7**, which is typical for a corroding metal. The parameters R_{ct} and Q_{dl} account for the properties of the reactions at the passive film/artificial saliva interface and their values are displayed in **Table 3**.

The observed behaviour suggests that the passive layers formed at the surface of Zr-Ag alloys more efficiently resist the onset of localized corrosion, in agreement with the results obtained from potentiodynamic polarization measurements.
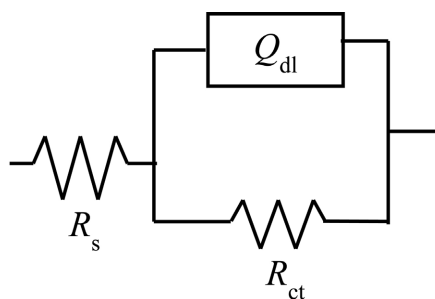
Figure 7. Proposed equivalent circuit for modeling experimental impedance data performed after polarization at +500 mV/SCE of cp Zr in artificial saliva, pH = 4.0.

Table 3. Electrical parameters of the equivalent circuits for cpZr and Zr-Ag alloys after polarization at +500 mV (SCE) in aerated artificial saliva, pH = 4.0, at 37˚C.

Sample	Q_p (10^5 S cm^{-2} s^{-n})	n_p	R_p (Ω cm²)	Q_b (10^5 S cm^{-2} s^{-n})	n_b	R_b (Ω cm²)	Q_{dl} (10^5 S cm^{-2} s^{-n})	n	R_{ct} (Ω cm²)
cpZr							2.8	0.85	2.1×10^4
Zr-1Ag	2.6	0.88	1.9×10^3	1.2	0.90	6.0×10^5			
Zr-3Ag	2.5	0.89	2.7×10^3	1.1	0.91	7.6×10^5			
Zr-5Ag	2.4	0.90	3.5×10^3	1.0	0.92	9.5×10^5			

The electrochemical results obtained in this study showed that silver is very effective in enhancing the corrosion resistance of zirconium, as evidenced by the increase in open circuit potential, breakdown potential and impedance values. Such increase in corrosion resistance is expected because Ag is a nobler element than Zr. Previous studies have shown that silver alloying additions improve the corrosion resistance of Ti by promoting spontaneous passivation in chloride-containing environments owing to enhanced cathodic reaction [24] [43]. The presence of silver at the solution/metal or solution/oxide/metal interface affects the kinetics of cathodic reaction on Zr by the following mechanisms: (a) increasing the exchange current density, i_0, and/or (b) reducing the cathodic Tafel slope, b_c. Therefore, the open circuit potential shifts to more noble values and the formed oxide film tends to thicken [44]. On the other hand, because of the higher electromotive force of silver compared to zirconium, Ag atoms may accumulate at the surface of Zr-Ag alloys during the initial stage of corrosion due to the preferential dissolution of Zr, thus promoting the formation of a more stable and compact passive film. As a result, the oxide film grown at the surface of Zr-Ag alloys exhibits improved barrier properties thereby exerting an effective inhibiting action towards the corrosion process.

4. Conclusions

The corrosion behaviour of three Zr-Ag alloys has been assessed in artificial saliva (pH = 4.0) in order to investigate their potential use as materials for dental applications. The development of passivity for all the investigated materials is

deduced from both open circuit potential measurements and potentiodynamic polarization curves, and the corrosion resistance of Zr-Ag alloys results from the development of a passive film at their surface.

Silver alloying additions reduce the susceptibility of zirconium towards localized corrosion, as evidenced by the shift of breakdown potential to more positive values. All Zr-Ag alloys exhibit pitting potentials higher than the potential values that may occur in the human body [29]. The potential for breakdown of the passive film achieved by all the investigated alloys can be regarded safe enough for these materials to be proposed for dental implant.

EIS measurements performed at the open circuit potential indicate that the oxide films formed at the surface of Zr-Ag alloys show better barrier properties compared to pure Zr. Such passive layers significantly inhibit the penetration of chloride ions, thus reducing the electrode corrosion rate. Moreover, impedance data obtained at potentials reported to be achieved in the human body for Ti implants highlight a thickening of these passive layers without the onset of localized corrosion phenomena, unlike what occurs on cp Zr where a thinning of the passive film or even losses of the film continuity due to localized corrosion reactions is observed.

Silver alloying additions not only promote the development of a thicker and more stable passive oxide film, but also increase its compactness, which contributes significantly to improve the corrosion resistance of Zr-Ag alloys.

Conflicts of Interest

The authors declare no conflicts of interest regarding the publication of this paper.

References

[1] Mehjabeen, A., Song, T., Xu, W., Tang, H.P. and Qian, M. (2018) Zirconium Alloys for Orthopaedic and Dental Applications. *Advanced Engineering Materials*, **20**, Article ID: 1800207. https://doi.org/10.1002/adem.201800207

[2] Yamamoto, A., Honma, R. and Sumita, M. (1998) Cytotoxicity Evaluation of 43 Metal Salts Using Murine Fibroblasts and Osteoblastic Cells. *Journal of Biomedical Materials Research*, **39**, 331-340.
https://doi.org/10.1002/(SICI)1097-4636(199802)39:2<331::AID-JBM22>3.0.CO;2-E

[3] Olmedo, D.G., *et al.* (2011) *In vivo* Comparative Biokinetics and Biocompatibility of Titanium and Zirconium Microparticles. *Journal of Biomedical Materials Research Part A*, **98**, 604-613.

[4] Guglielmotti, M.B., Cabrini, R.L. and Guerrero, C. (1994) A Method for the Quality Control of Osseointegration in Endosseous Implants. *Acta odontológica Latinoamericana*, **8**, 9-14.

[5] Guglielmotti, M.B., Cabrini, R.L. and Renou, S. (1999) A Histomorphometric Study of Tissue Interface by Laminar Implant Test in Rats. *The International Journal of Oral & Maxillofacial Implants*, **14**, 565-570.

[6] Kulokaov, O.B., Doktorov, A.A., D'iakova, S.V., Denisov-Nikol'skii, I.I. and Grotz, K.A. (2005) Experimental Study of Osseointegration of Zirconium and Titanium

Dental Implants. *Morfologiia*, **127**, 52-55.

[7] Kohn, D.H. (1998) Metals in Medical Applications. *Current Opinion in Solid State and Materials Science*, **3**, 309-316. https://doi.org/10.1016/S1359-0286(98)80107-1

[8] Patel, A.M. and Spector, M. (1997) Tribological Evaluation of Oxidized Zirconium Using an Articular Cartilage Counterface: A Novel Material for Potential Use in Hemiarthroplasty. *Biomaterials*, **18**, 441-447.
https://doi.org/10.1016/S0142-9612(96)00152-4

[9] Chaturvedi, T.P. (2009) An Overview of the Corrosion Aspect of Dental Implants (Titanium and Its Alloys). *Indian Journal of Dental Research*, **20**, 91-98.
https://doi.org/10.4103/0970-9290.49068

[10] Green, N.T. (2002) Fracture of Dental Implants: Literature Review and Report of a Case. *Implant Dentistry*, **11**, 137-143.
https://doi.org/10.1097/00008505-200204000-00014

[11] Gomez-Florit, M., Xing, R. and Ramis, J.M. (2014) Differential Response of Human Gingival Fibroblasts to Titanium- and Titanium-Zirconium-Modified Surfaces. *Journal of Periodontal Research*, **49**, 425-436.

[12] Fahey, J., Holmes, D. and Yau, T.-L. (1997) Evaluation of Localized Corrosion of Zirconium in Acidic Chloride Solutions. *Corrosion*, **53**, 54-61.
https://doi.org/10.5006/1.3280434

[13] Rosalbino, F., Macciò, D., Saccone, A. and Delfino, S. (2012) Stability of the Passive State of Zr–Nb Crystalline Alloys. *Materials and Corrosion*, **63**, 580-585.
https://doi.org/10.1002/maco.201006012

[14] Baboian, R. (1995) Corrosion Tests and Standards: Application and Interpretation. ASTM, Philadelphia.

[15] Al-Mayouf, A.M., Al-Swayih, A.A., Al-Mobarak, N.A. and Al-Jabab, A.S. (2004) Corrosion Behavior of a New Titanium Alloy for Dental Implant Applications in Fluoride Media. *Materials Chemistry and Physics*, **86**, 320-329.
https://doi.org/10.1016/j.matchemphys.2004.03.019

[16] Zhang, B.B., Wang, B.L., Li, L. and Zheng, Y.F. (2011) Introduction of Antibacterial Function into Biomedical TiNi Shape Memory Alloy by the Addition of Element Ag. *Acta Biomaterialia*, **7**, 2758-2767.

[17] Takahashi, M., Kikuchi, M., Yakada, Y., Okabe, T. and Okuno, O. (2006) Electrochemical Behavior of Cast Ti-Ag Alloys. *Dental Materials Journal*, **3**, 516-523.
https://doi.org/10.4012/dmj.25.516

[18] Rosalbino, F., Delsante, S., Borzone, G. and Scavino, G. (2012) Influence of Noble Metals Alloying Additions on the Corrosion Behaviour of Titanium in a Fluoride-Containing Environment. *Journal of Materials Science: Materials in Medicine volume*, **23**, 1129-1137. https://doi.org/10.1007/s10856-012-4591-9

[19] Robert, G.C., O'Brien, W.J. and Powers, J.M. (1992) Dental Materials: Properties and Manipulation. Mosby-Years Book, Missouri.

[20] Zheng, Y.F., Wang, B.F., Wang, J.G., Li, C. and Zhao, L.C. (2006) Optimization of Mechanical Properties, Biocorrosion Properties and Antibacterial Properties of as-Cast Ti–Cu Alloys. *Materials Science and Engineering C*, 26, 14-19.

[21] Cremasco, A., Osorio, W.R., Freire, C.M.A., Garcia, A. and Caram, R. (2008) Electrochemical Corrosion Behavior of a Ti-35Nb Alloy for Medical Prostheses. *Electrochimica Acta*, **53**, 4867-4874. https://doi.org/10.1016/j.electacta.2008.02.011

[22] Oliveira, N.T.C., Biaggio, S.R., Rocha-Filho, R.C. and Bocchi, N. (2005) Studies on the Stability of Anodic Oxides on Zirconium Biocompatible Alloys. *Journal of Bio-*

medical Materials Research, **39**, 397-407. https://doi.org/10.1002/jbm.a.30352

[23] Shukla, A.K. and Balasubramaniam, R. (2006) Effect of Surface Treatment on Electrochemical Behavior of CP Ti, Ti–6Al–4V and Ti–13Nb–13Zr Alloys in Simulated Human Body Fluid. *Corrosion Science*, **48**, 1696-1720. https://doi.org/10.1016/j.corsci.2005.06.003

[24] Zhang, B.B., Zheng, Y.F. and Liu, Y. (2009) Optimization of Mechanical Properties, Biocorrosion Properties and Antibacterial Properties of As-Cast Ti–Cu Alloys. *Dental Materials*, **25**, 467-472.

[25] Lavos-Valereto, I.C., Costa, I. and Wolynec, S. (2002) The Electrochemical Behavior of Ti-6Al-7Nb Alloy with and without Plasma-Sprayed Hydroxyapatite Coating in Hank's Solution. *Journal of Biomedical Materials Research*, **63**, 664-670. https://doi.org/10.1002/jbm.10351

[26] de Assis, S.L., Wolynec, S. and Costa, I. (2006) Corrosion Characterization of Titanium Alloys by Electrochemical Techniques. *Electrochimica Acta*, **51**, 1815-1819. https://doi.org/10.1016/j.electacta.2005.02.121

[27] Rostomov, N., Judge, W. and Jarjoura, G. (2020) Electrochemical Behavior of Alumix 321 PM and AA6061 Alloys in 3.5 wt% NaCl Solution by Electrochemical Impedance Spectroscopy Measurements. *Journal of Materials Science and Chemical Engineering*, **8**, 42-49. https://doi.org/10.4236/msce.2020.810005

[28] Scully, J.R. and Kelly, R.G. (2003) ASM Handbook. vol. 13, ASM International, Materials Park, OH.

[29] Rondelli, G. and Vicentini, B. (2002) Effect of Copper on the Localized Corrosion Resistance of Ni-Ti Shape Memory Alloy. *Biomaterials*, **23**, 639-644. https://doi.org/10.1016/S0142-9612(01)00142-9

[30] Wang, L.-N. and Luo, J.-L. (2012) Electrochemical Behaviour of Anodic Zirconium Oxide Nanotubes in Simulated Body Fluid. *Applied Surface Science*, **258**, 4830-4833. https://doi.org/10.1016/j.apsusc.2012.01.043

[31] Zhou, F.Y., Wang, B.L., Qiu, K.J, Lin, W.J., Li, L., Wang, Y.B., Nie, F.L. and Zheng, Y.F. (2012) Microstructure, Corrosion Behavior and Cytotoxicity of Zr–Nb Alloys for Biomedical Application. *Materials Science and Engineering: C*, **32**, 851-857. https://doi.org/10.1016/j.msec.2012.02.002

[32] Pauportè, T. and Finne, J. (2006) Impedance Spectroscopy Study of Anodic Growth of Thick Zirconium Oxide Films in H_2SO_4, Na_2SO_4 and NaOH Solutions. *Journal of Applied Electrochemistry*, **36**, 33-41. https://doi.org/10.1007/s10800-005-9011-0

[33] Gomez Sanchez, A., Schreiner, W., Duffò, G. and Cerè, S. (2011) Surface Characterization of Anodized Zirconium for Biomedical Applications. *Applied Surface Science*, **257**, 6397-6405. https://doi.org/10.1016/j.apsusc.2011.02.005

[34] Mareci, D., Bolat, G., Cailean, A., Santana, J.J., Izquierdo, J. and Souto, R.M. (2014) Effect of Acidic Fluoride Solution on the Corrosion Resistance of ZrTi Alloys for Dental Implant Application. *Corrosion Science*, **87**, 334-343. https://doi.org/10.1016/j.corsci.2014.06.042

[35] Assis, S.L. and Costa I. (2007) Electrochemical Evaluation of Ti-13Nb-13Zr, Ti-6Al-4V and Ti-6Al-7Nb Alloys for Biomedical Application by Long-Term Immersion Tests. *Materials and Corrosion*, **58**, 329-333. https://doi.org/10.1002/maco.200604027

[36] Liao, X., Kong, X., Dong, P. and Chen, K. (2020) Effect of Pre-Aging, Over-Aging and Re-Aging on Exfoliation Corrosion and Electrochemical Corrosion Behavior of Al-Zn-Mg-Cu Alloys. *Journal of Materials Science and Chemical Engineering*, **8**, 81-88. https://doi.org/10.4236/msce.2020.82008

[37] Aziz-Kerzo, M., Conroy, K.G., Fenelon, A.M., Farrel, S.T. and Breslin, C.B. (2001) Electrochemical Studies on the Stability and Corrosion Resistance of Titanium-Based Implant Materials. *Biomaterials*, **22**, 1531-1539. https://doi.org/10.1016/S0142-9612(00)00309-4

[38] Gudic, S., Radosevic, J. and Kliskic, M.K. (2002) Study of Passivation of Al and Al-Sn Alloys in Borate Buffer Solutions Using Electrochemical Impedance Spectroscopy. *Electrochimica Acta*, **47**, 3009-3016. https://doi.org/10.1016/S0013-4686(02)00246-3

[39] Orazem, M. and Tribollet, B. (2007) Electrochemical Impedance Spectroscopy. Wiley, New York. https://doi.org/10.1002/9780470381588

[40] Oskarsson, M., Ahlberg, E. and Petterson, K. (2001) Oxidation of Zircaloy-2 and Zircaloy-4 in Water and Lithiated Water at 360°C. *Journal of Nuclear Materials*, **295**, 97-108. https://doi.org/10.1016/S0022-3115(01)00480-9

[41] Vasquez, G. and Gonzalez, I. (2007) Diffusivity of Anion Vacancies in WO_3 Passive Films. *Electrochimica Acta*, **52**, 6771-6777. https://doi.org/10.1016/j.electacta.2007.04.102

[42] Olsson, C.O.A. and Landolt, D. (2003) Anodisation of a Nb–Zr Alloy. *Electrochimica Acta*, **48**, 3999-4011. https://doi.org/10.1016/S0013-4686(03)00540-1

[43] Takada, Y., Nakajima, H., Okuno, O. and Okabe, T. (2001) Released Ions and Microstructures of Dental Cast Experimental Ti-Ag Alloys. *Dental Materials Journal*, **20**, 34-52. https://doi.org/10.4012/dmj.20.34

[44] Blackwood, S., Chua, A.W.C., Seah, K.H.W., Thampuran, R. and Teoh, S.H. (2000) Corrosion Behaviour of Porous Titanium-Graphite Composites Designed for Surgical Implants. *Corrosion Science*, **42**, 481-503. https://doi.org/10.1016/S0010-938X(99)00103-1